Experimental Evaluation of Forward Error Correction Techniques for High-Rate Underwater Acoustic Communication Systems

Deniz Unal[1], Kerem Enhos[1], Emrecan Demirors[1], and Tommaso Melodia[1]

[1]Institute for the Wireless Internet of Things, Northeastern University, Boston, MA 02115

Email: {enhos.k, e.demirors, unal.d, melodia}@northeastern.edu

Abstract: *Forward Error Correction (FEC) is a well-established technique to enhance communication links' reliability in various domains. In underwater acoustic communications, using FEC is particularly crucial, as retransmissions are impractical and may lead to reduced throughput, increased latency, and decreased energy efficiency. However, FEC schemes may perform poorly under frequency-dependent channel attenuation and temporal and spatial channel variability, leading to non-uniform bit error distribution. Furthermore, in practical underwater systems, this issue is amplified due to diverse acoustic noise sources and the non-ideal behavior of the hardware. In this work, we analyze the distribution of errors on a wideband orthogonal frequency-division multiplexing (OFDM) system with larger number of subcarriers compared to terrestrial wireless communication systems. Specifically, we investigate the impact of frequency-dependent channel attenuation and temporal and spatial channel variability on the distribution of bit errors in the underwater OFDM system. Integration of block codes, convolutional codes, turbo codes, low-density parity-check codes, and polar codes to the underwater zero-padded OFDM system is described in detail. We explain the design principles and operation of each type of code and discuss their suitability for underwater communication systems. We also describe the process of integrating these codes into the underwater OFDM system and the modifications required to adapt the codes to the unique characteristics of underwater channels. We perform experiments in a real-world underwater environment to evaluate the effectiveness of the FEC schemes in improving the reliability of underwater communication. We vary the signal-to-noise ratio to generate different levels of channel noise and evaluate the performance of each FEC scheme in terms of its ability to correct errors and maintain data throughput. Through experimental results, we compare the performance of different FEC schemes in terms of computational efficiency, latency, and adaptability.*

Keywords: *underwater acoustic communications, forward error correction (FEC), orthogonal frequency-division multiplexing (OFDM).*

1. INTRODUCTION

The significance of employing Forward Error Correction (FEC) techniques to enhance the reliability of communication links is widely recognized across various domains. In the domain of underwater acoustic communications, the utilization of FEC holds particular importance, as the feasibility of retransmissions is limited, potentially resulting in reduced throughput, increased latency, and decreased energy efficiency. This importance is even further amplified in the case of establishing high-rate underwater acoustic links where relatively larger bandwidths (e.g., $>$ 100 kHz) need to be leveraged efficiently. However, FEC schemes may exhibit inadequate performance in the face of frequency-dependent channel attenuation, as well as temporal and spatial channel variability inherent in underwater environments, thereby leading to non-uniform distributions of bit errors.

The main indication of these errors is the fluctuating signal-to-noise ratio (SNR) resulting from varying received signal levels within the bandwidth. The source of these errors can be attributed to both the acoustic channel and the system design. Location and frequency-dependent effects such as path loss, various acoustic noise such as wind and shipping noise, and multipath are the fundamental sources of errors for the acoustic channel [1]. On the system side, imperfections such as frequency responses of transducers on both transmit and receive nodes SNR levels. Another imperfection is the nonlinearity in the transmitter and receiver amplifier chains which may cause distortion and performance degradation in certain parts of the frequency band. This is particularly an issue if large bandwidths are utilized for communication. A typical example case occurs if harmonic content is in-band such that $f_{\mathrm{H}} \geq N f_{\mathrm{L}};\ N \in \{2, 3, \dots\}$ where f_{L} and f_{H} correspond to lowest and highest frequency of the system.

The presence of diverse natural and man-made acoustic noise sources is another major factor behind the non-uniform bit errors. In contrast to the RF spectrum, the underwater acoustic spectrum lacks regulatory measures for device access and usage. Consequently, a wide range of devices, such as communication devices, passive and active SONAR systems used in seismology, profiling, exploration, and navigation, exploit spectrum resources without restrictions on frequency or power. Additionally, it is essential to acknowledge that marine animals themselves possess the capacity to utilize spectrum resources [1]. To provide a real-world example to the aforementioned factors, an example power spectrum density of the recorded noise sources at the experiment location (Boston Harbor) in a time period when shipping and boating activity is relatively low, depicted in Figure 1 (left). Figure 1 (right) depicts a snapshot from this recording. This short recording proves the presence of diverse and wideband acoustic noise sources in the spectrum.

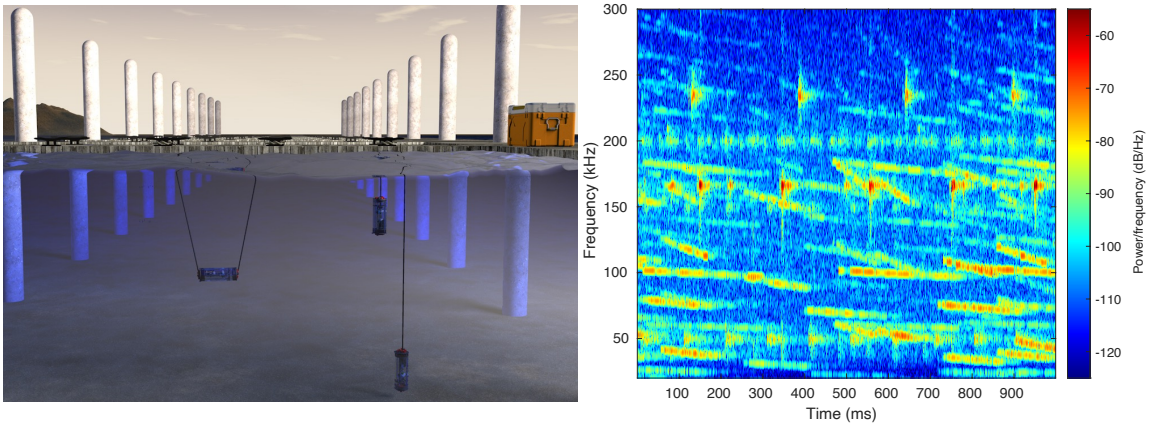

Figure 1: Deployment setting (left). Spectrogram of an ambient noise recording in deployment location (right).

The literature has extensively examined the performance of channel coding for underwater acoustic communications. In [2], a comparative analysis was conducted, utilizing Convolu-

tional, Reed-Solomon, and turbo product codes, through an experimental investigation involving a QPSK-based modem designed for image transmission. The performance evaluation in [3] encompasses various channel coding techniques compiled from diverse sources, including Polar, LDPC, and Reed-Solomon PSK modulated link. Additionally, [4] presents a comprehensive experimental study on coding for single carrier systems in arctic environments. These studies primarily concentrate on single-carrier systems, with a focus on limited bandwidth utilization. In this work, the emphasis is placed on a wideband, multicarrier platform for achieving high data rates in underwater acoustic communications. A detailed experimental study is presented, wherein the error correction performance of various FEC codes including BCH, LPDC, Polar, Convolutional, and Turbo Codes are evaluated and compared.

The paper is structured as follows. Section 2 introduces the system design and provides an overview of multi-carrier communication and channel coding. Section 3 describes the experimental setup, including system configuration and test procedure. Section 4 presents the experimental results. Finally, Section 5 concludes the paper.

2. SYSTEM DESCRIPTION

In this section, first, the communication system that is considered for establishing high-rate underwater acoustic communication systems is described. Consequently, the FEC coding methods that are evaluated and assumptions made for their implementations are described.

Communication System. The multi-carrier communication scheme (i.e., Zero-Padded Orthogonal Frequency Division Multiplexing (OFDM) (ZP-OFDM)) is selected due its proven performance in supporting high-rate acoustic links in underwater [5, 6]. A ZP-OFDM block with K subcarriers, B bandwidth, and a duration of $T = 1/B$ is considered.

$$s(t) = Re\left\{\sum_{k=0}^{K-1} a_k \mathrm{e}^{j2\pi f_k t}\right\}, t \in [0, T], \tag{1}$$

where a_k denotes the symbol in subcarrier k with corresponding frequency $f_k = f_0 + kB/K$. The symbols are assigned equally spaced N_p pilot symbols with indices k_p, and $N_d = K - N_p$ data symbols denoted with d_n with indices $n \in \{0, \ldots, N_d - 1\}$ between pilots. On the receiver algorithm, as detailed in [5, 6], first, pilot symbols are utilized to obtain channel estimates which are then processed with zero-forcing equalizer to recover data symbols. For packet detection and synchronization and Doppler estimation and compensation, each ZP-OFDM packet was preceded with a preamble and followed with a postamble based on single linear frequency modulated (LFM) pulses. Moreover, an additional preamble sequence consisting of a pseudo-random noise (PN) sequence precedes the packet to further improve the packet detection and synchronization capabilities, as in [7]. To evaluate the performance of the system, bit-error-rate (BER) measured across subcarriers and packets are considered. For instance, for BPSK mapped data symbols, a bit error is $e_n = 1$ if $d_k^{RX} \neq d_k^{TX}$ and $e_n = 0$ otherwise. Consequently, subcarrier (BER_n) and packet BERs (BER) is measured as:

$$\text{BER}_n = \frac{1}{M}\sum_{m=1}^{M} e_n^m;\ n \in \{0, \ldots, N_d - 1\}, \tag{2}$$

$$\text{BER} = \frac{1}{MN_d}\sum_{m=1}^{M}\sum_{n=0}^{N_d-1} e_n^m. \tag{3}$$

A real-world example of the distribution of bit errors over a short duration of packets ($\sim 10^5$ bits) is presented in Figure 2 to illustrate practical implementation. On the x-axis, the OFDM subcarrier indices (for data subcarriers) are shown, and on the y-axis, the subcarrier BER (BER_n) is given. The performance of two different spatially and temporally similar channels

with minor differences is compared in this figure. Two modems are deployed as receivers at the same distance (i.e., 7,m) from a third, transmitter modem with different orientations. As shown in 1 (left), while the first receiver modem is deployed in a vertical orientation directly facing down towards the transmitter node, the second receiver is deployed in a horizontal orientation relative to the transmitter node. The differences in the distribution of flipped bits can be observed in line with the previous discussion about the effect of modem location and equipment. These bits will be subjected to forward error correction techniques.

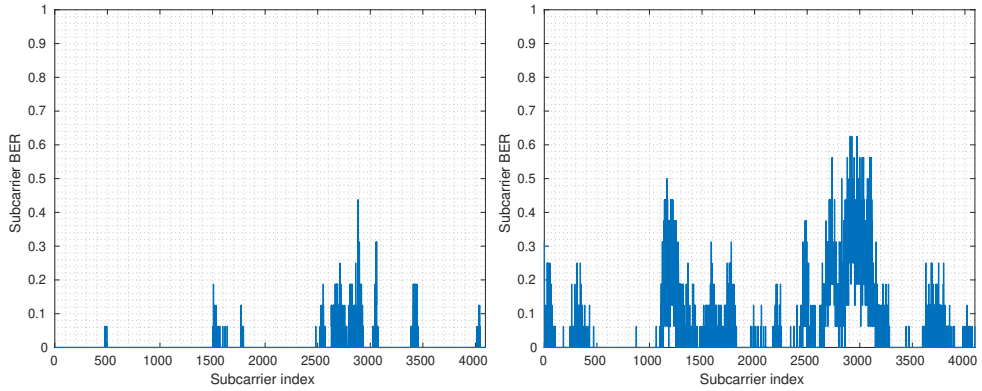

(a) Vertically Deployed Receiver. *(b) Horizontally Deployed Receiver.*

Figure 2: Distribution of bit errors to OFDM subcarriers.

FEC Coding. FEC coding provides reliable transmission over unreliable channels by adding redundancy to information bits to produce codewords. The decoder then corrects distortion caused by the channel with the help of redundancy bits. The amount of introduced redundancy is characterized is defined as the code rate R, the ratio of information bits to codeword bits. In this paper five FEC coding schemes from block code and convolutional code classes are implemented and evaluated.

BCH is the first block code considered in this paper [8]. The encoding operation of BCH codes uses a generator polynomial similar to other cyclic codes while Berlekamp's algorithm is used for the decoding operation. It is possible to derive worst-case error correction capability in terms of bits for a given BCH code and therefore it can be used as a benchmark. In this work, narrow-sense BCH codes over binary fields for the given code rates are used. LDPC is a popular high-performance channel coding scheme used in 5G NR and DVB. LDPC codes are defined with sparse parity-check matrices [9]. To generate the parity-check matrix for desired code rates and number of data symbols progressive edge growth algorithm is used. The decoding of the received LDPC packets is performed with belief propagation algorithm. Polar codes is another block code scheme introduced relatively recently [10] and widely used in 5G NR. The encoding algorithm performs channel polarization using polar transformation to map data and frozen bits to codewords. In this work, the decoder used is based on successive cancellation algorithm.

Convolutional codes are another well-established class of codes [11]. The encoder implements convolution operation on information bits using shift registers and which can be described with a trellis structure. On the decoder side, the Viterbi algorithm is used to find the most probable input bits for a given codeword. In this implementation, a constraint length of 12 is used along with zero-bit termination. Finally, the parallel concatenated convolutional codes known as turbo coding [12] is also considered. The structure consists of two identical convolutional encoders with an interleaver between them in addition to a systematic output. The error correction capability of this code is affected by its interleaver structure. In this work, a random interleaver between two encoders (optimal selection of an interleaver structure is beyond the scope of this paper), a memory of 3 for encoders with a code rate $1/3$ and data streams terminated with 12 tail bits are considered. The input to the encoder is set to be data subcarriers of each ZP-OFDM block with no partitioning and hard decision mechanism is used. Moreover, since burst errors are expected on the received packets, a helical scan interleaver is added after

channel encoding step to make subcarrier error distribution more uniform. The implementation is similar to a typical matrix interleaver but each row is circularly shifted with incrementing steps. On the receiver side, the bit ordering is inverted with a deinterleaver.

3. EXPERIMENTAL SETTING

Performance evaluation study for different FEC coding schemes are conducted in Charlestown Marina, MA, USA. Different FEC schemes are implemented and tested by using a COTS software-defined underwater modem, the Hydronet Wideband Modular Modem (WMM) [13]. Thanks to the Hydronet WMM's software-defined capabilities, including a native GNU Radio Driver, custom waveforms and FEC schemes are generated, transmitted and received/recorded. While Hydronet Modems offer the capability to implement and realize various software-defined transceivers on the device, for this study, their transmitting and recording features are utilized. Particularly, the data collection process is performed using pre-generated packets and subsequently transmitting and recording them over the acoustic channel with varying transmit power levels. The recorded packets are processed offline for detailed performance evaluation. The packets are sequentially transmitted and recorded following the procedure in [14]. In terms of deployment setting, as shown in Fig 1 (left), two modems which are deployed vertically through the docks with transducers facing each other at a separation of approximately 10 meters, are used for the experiments.

In the experiments, as explained in Section 2, a ZP-OFDM communication scheme is used. Specifically, ZP-OFDM packets utilize a total of 8192 subcarriers, out of which 1365 and 4095 are dedicated to pilot and data symbols, respectively. The remaining subcarriers are null and not loaded with any symbols. Data and pilot symbols are modulated with BPSK mapping scheme. This configuration results in effective OFDM bandwidth of 104.14 kHz and the corresponding subcarrier bandwidth is 19.07 Hz. The bit rate of system is approximately 38.8 kbps. The center frequency of the system is selected as 125 kHz based on transducer responses and bandwidth requirements. To sufficiently overcome any inter-block-interference among OFDM blocks due to the multipath effect, a guard interval duration of 25 ms is selected. This duration is significantly longer than the multipath spread of the channel which is measured in a prior channel measurement study. For channel coding, error correction coding schemes that are detailed in Section 2 is used with varying code rates.

The parameters for coding are determined for the number of data subcarriers according to Sec. 2. In the case of convolutional and turbo codes, some bits are assigned for termination. In polar-coded packets, block size requires one more bit than the size of data subcarriers and for simplification, we assume that this bit is lost and randomly assigned in the receiver algorithm. To ensure a fair comparison, equal code rates are targeted for each coding scheme in all cases. As a result, the actual payload sizes may vary slightly between the different coding schemes. However, when it comes to throughput, the difference is negligible. In this study, it is assumed that source coding has already been performed, and as a result, message bits are pseudorandomly generated at the transmitter side. The known seed at the receiver allows message reconstruction for bit error analysis. The packet error rate and error correction assessment utilize a multi-step procedure. Before transmission, the payload generated is subjected to encoding using the selected FEC coding configuration, followed by mapping to OFDM subcarriers. The mapping process may involve additional procedures such as zero padding or interleaving. Both the generated source payload and the encoded payload are saved. Upon transmitting packets through the channel and receiving them, their payloads are retrieved after performing detection and synchronization. It is important to note that, at this stage, deinterleaving is not applied in order to maintain the bit-to-subcarrier assignment. The calculation of the bit error rate (BER) at this stage pertains to error levels without channel coding. The received bits undergo demapping and FEC decoding operations. The coded BER is then determined by comparing the original generated payload prior to encoding with the received and decoded payload.

4. EXPERIMENTAL RESULTS

In this section, different codes and code rates are evaluated in terms of performance, using the experimental setting detailed in Section 3.

First, average BERs with respected to transmission (TX) gain levels are measured for different codes and code rates. As shown in Fig. 1 (right), the presence of multiple active noise sources in the deployment location caused the signal-to-noise SNR levels fluctuate heavily even among consecutive packets. Therefore, in the experiments, to evaluate different codes and code rates with a controllable benchmark metric, TX gain level is selected. Average BERs with respect to TX gain levels can be observed in in Figures 3, 4, and 5 for code rates $1/3$, $1/2$, and $2/3$, respectively. In the case of $R = 1/3$, it can be observed that errors can be corrected by every channel coding at higher TX gain levels. In terms of overall performance, Turbo coding emerges as the most prominent coding scheme, followed by Convolutional coding. LDPC and Polar codes demonstrate comparable performance, while BCH experiences rapid degradation with an increasing number of errors. In the case of $R = 1/2$, the minimum transmit power level required to achieve error-free packets exhibits an increase of approximately 6 dB compared to the $R = 1/3$ case. Below -21,dB, the effectiveness of all coding scheme diminish. Among the coding schemes, LDPC demonstrated the highest performance, followed by Polar and BCH. At this rate, Convolutional coding demonstrated effectiveness primarily at higher transmit levels, but it failed to improve reliability as the TX power level and consequently the SNR level, decreased. With an increase in code rate to $2/3$, it is anticipated that the performance of FEC coding would decline. At this rate, LDPC exhibited the ability to correct the highest number of bit errors, although most packets still contained errors. Similar to the $R = 1/2$ case, Polar and BCH outperformed Convolutional coding, which showed poor performance.

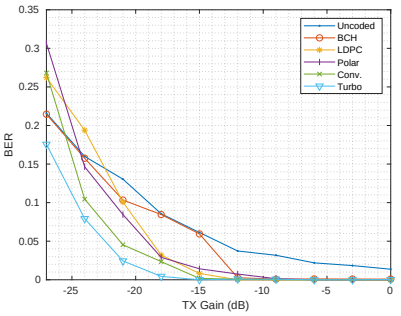

Figure 3: TX Gain vs BER for $R = 1/3$

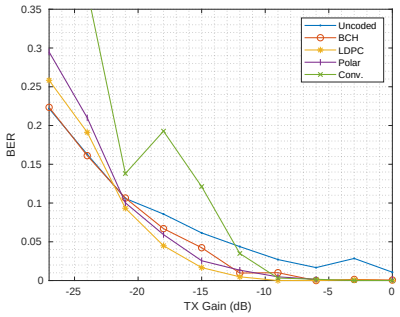

Figure 4: TX Gain vs BER for $R = 1/2$

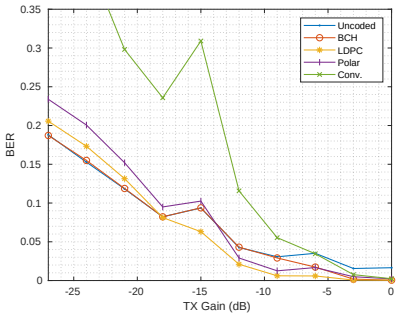

Figure 5: TX Gain vs BER for $R = 2/3$

In the second part of the performance evaluation study, the focus was shifted towards comprehending the maximum error correction capability of each FEC code in the selected experimental configuration. Table 1 presents the maximum BER that can be corrected using different coding schemes with different rates both with and without an interleaver. These values could serve as the estimated FEC limit, representing the upper bound of achievable error correction performance in this configuration. Overall, as expected, increasing the code rate decreases the upper bound of error correction capability. For instance, Convolutional codes with an interleaver can correct packets possess approximately 13% and 3% erroneous bits at the rates $R = 1/3$ and $R = 2/3$, respectively. Another important observation is that Convolutional and Polar Codes can significantly benefit from incorporating interleavers in improving their FEC limits. For instance, both Convolutional and Polar Codes can have more than one order of magnitude better FEC limits at almost all code rates. For the case of BCH codes, the error correction performance of the code rate can be derived as explained in Section 2.

Finally, in Fig. 6, subcarrier error distribution over time is shown for a recording, where the x-axis denotes packet indices and blue marks correspond to bit flips at a given subcarrier. Fig. 6a is the map of errors before the deinterleaver block and Fig. 6b shows how errors are

	w/ Interleaver			w/o Interleaver		
	R=1/3	**R=1/2**	**R=2/3**	**R=1/3**	**R=1/2**	**R=2/3**
BCH	7.47×10^{-2}	4.76×10^{-2}	2.83×10^{-2}	7.47×10^{-2}	4.84×10^{-2}	2.91×10^{-2}
LDPC	9.38×10^{-2}	7.84×10^{-2}	4.32×10^{-2}	1.03×10^{-1}	9.01×10^{-2}	4.71×10^{-2}
Polar	1.03×10^{-1}	6.50×10^{-2}	2.76×10^{-2}	4.52×10^{-2}	1.88×10^{-2}	4.88×10^{-3}
Conv.	1.34×10^{-1}	7.99×10^{-2}	2.95×10^{-2}	5.10×10^{-2}	1.10×10^{-2}	3.91×10^{-3}
Turbo	1.23×10^{-1}	N/A	N/A	7.69×10^{-2}	N/A	N/A

Table 1: Estimated FEC limits for channel codes at different rates with and without interleaver

distributed after deinterleaving and before the channel decoding operation. It can be observed that, in addition to occasional random bit errors scattered around the spectrum, most of the errors are concentrated around certain frequencies. The effect of noise sources described in Sec. 1 can be observed, such as the periodic pulse close to 170 kHz. In this recording, mean BER without coding is measured to be 4.53×10^{-2}, equivalent to 186 flipped bits on average.

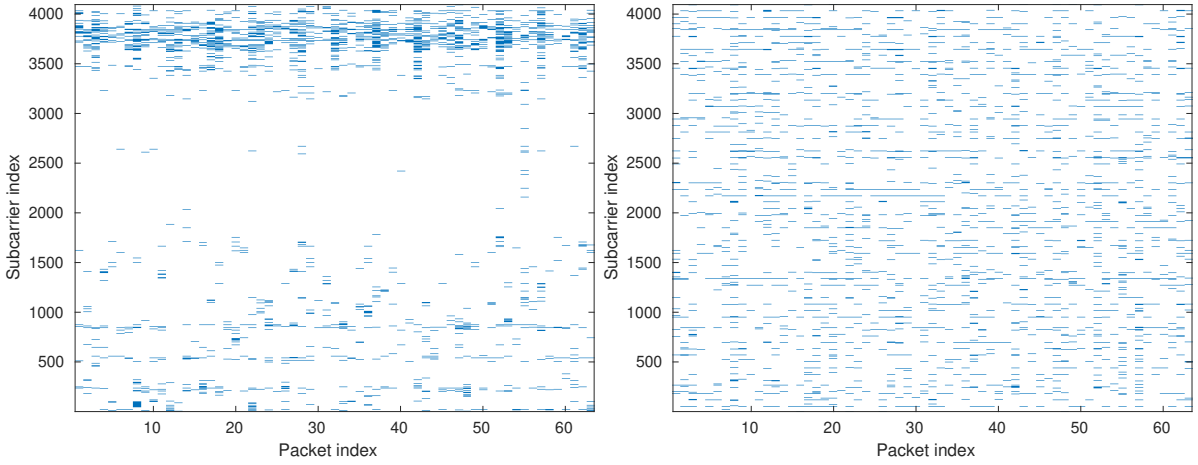

(a) Before deinterleaver *(b) After deinterleaver*

Figure 6: Packet-by-packet distribution of bit errors over OFDM subcarriers prior without channel coding

5. CONCLUSIONS

In this paper, forward error correction in wideband, multicarrier underwater acoustic communication systems used to establish high-data rate links is evaluated. Error sources are identified based on system design and external noise sources at a shallow deployment scenario with marine activity. Finally, error correction capabilities of BCH, LDPC, Polar, Convolutional, and Turbo codes are demonstrated and compared with an experimental study conducted at sea using software-defined underwater acoustic modems. The effect of interleaver is shown and upper limits of error correction capabilities is illustrated.

6. ACKNOWLEDGEMENTS

This work was supported by the National Science Foundation under Grant CNS-1763964 and Grant CNS-1726512.

REFERENCES

[1] T. Melodia et al. “Advances in Underwater Acoustic Networking”. In: *Mobile Ad Hoc Networking: Cutting Edge Directions*. Ed. by S. Basagni et al. 2nd. Inc., Hoboken, NJ: John Wiley and Sons, 2013, pp. 804–852.

[2] J. Trubuil, A. Goalic, and N. Beuzelin. “An overview of channel coding for underwater acoustic communications”. In: *Prof. of IEEE MILCOM*. 2012, pp. 1–7.

[3] M. Falk, G. Bauch, and I. Nissen. “On Channel Codes for Short Underwater Messages”. In: *Information* 11.2 (2020).

[4] K. Pelekanakis, A. Alvarez, and J. Alves. “Comparison of Coded Modulation for Short Messages over High North Underwater Acoustic Channels”. In: *Proc. of ACM WUWNet*. WUWNet ’22. Boston, MA, USA, 2022.

[5] B. Li et al. “Multicarrier Communication Over Underwater Acoustic Channels With Nonuniform Doppler Shifts”. In: *IEEE Journal of Oceanic Engineering* 33.2 (Apr. 2008), pp. 198–209.

[6] E. Demirors et al. “A High-Rate Software-Defined Underwater Acoustic Modem with Real-Time Adaptation Capabilities”. In: *IEEE Access* PP.99 (2018), pp. 1–1. DOI: 10.1109/ACCESS.2018.2815026.

[7] D. Unal et al. “Field Experiments with Doppler Compensation in High-Frequency Underwater Acoustic Communication System”. In: *Proc. of IEEE ICC*. Rome, Italy, May 2023.

[8] R. Bose and D. Ray-Chaudhuri. “On a class of error correcting binary group codes”. In: *Information and Control* 3.1 (1960), pp. 68–79. ISSN: 0019-9958.

[9] R. Gallager. “Low-density parity-check codes”. In: *IRE Transactions on Information Theory* 8.1 (1962), pp. 21–28.

[10] E. Arikan. “Channel Polarization: A Method for Constructing Capacity-Achieving Codes for Symmetric Binary-Input Memoryless Channels”. In: *IEEE Transactions on Information Theory* 55.7 (2009), pp. 3051–3073.

[11] J. G. Proakis. *Digital communications*. McGraw-Hill, Higher Education, 2008.

[12] C. Berrou, A. Glavieux, and P. Thitimajshima. “Near Shannon limit error-correcting coding and decoding: Turbo-codes. 1”. In: *Proc. of IEEE ICC*. Vol. 2. 1993, 1064–1070 vol.2.

[13] Hydronet. URL: http://www.hydronet.tech.

[14] D. Uvaydov et al. “Sonair: Real-Time Deep Learning For Underwater Acoustic Spectrum Sensing and Classification”. In: *Proc. of DCOSS-IoT*. Pafos, Cyprus, June 2023.